

Application of Multiple-Input/Single-Output Analysis Procedures to Flight Test Data

J. K. Sridhar*

National Aeronautical Laboratory, Bangalore, 560 017 India

and

G. Wulff†

Deutsche Forschungsanstalt für Luft- und Raumfahrt, Braunschweig, D-3300 Germany

A computer program for the analysis of correlated multiple-input/single-output systems has been developed using the techniques of Bendat. This iterative procedure allows spectral separation to enable sequential as well as combined inspection of input/output relationships. The analogy of conditioning of spectral density functions to that of Gaussian elimination has been used for efficient realization of the algorithm. Described are the method and its applications to flight test data of two research vehicles, a helicopter and a new in-flight simulator. The examples show the detection of extraneous noise at the output caused by a fewer number of inputs together with the investigation of the control buildup in the helicopter case, and in the other case the influence of the autotrim system of the in-flight simulator on its direct lift control flaps. The results and conclusions are drawn based on the investigation of spectra and coherence functions.

Nomenclature

a_z	= normal acceleration (output signal)
$F_{xy}(f)$	= frequency response function of input $x(t)$ and output $y(t)$
f	= frequency
L_{rj}	= conditioned frequency response function
$N(f)$	= finite Fourier transform of noise $n(t)$
$n(t)$	= noise
p	= roll rate (output signal)
q	= number of inputs
r	= conditioning parameter
S_{ii}	= autospectrum of x_i
S_{ij-r}	= conditioned autospectrum
S_{ij}	= cross spectrum of x_i and x_j ($i \neq j$)
S_{ij-r}	= conditioned cross spectrum ($i \neq j$)
$S_{nn}(f)$	= noise spectrum
$S_{xx}(f)$	= autospectrum of input $x(t)$
$S_{xy}(f)$	= cross spectrum of input $x(t)$ and output $y(t)$
$S_{yy}(f)$	= autospectrum of output $y(t)$
T	= record length (time)
t	= time
$X(f)$	= finite Fourier transform of input $x(t)$
$X^*(f)$	= complex conjugate of $X(f)$
X_i	= finite Fourier transform of x_i
X_i^*	= complex conjugate of X_i
X_{i-r}	= ordered conditioned record $X_{i,12...r}$; that is, the linear effects of the first r records X_1, X_2, \dots, X_r ($r < i$) are removed from X_i
$x(t)$	= input record
x_i	= input record ($i = 1, 2, \dots, q$)
x_{q+1}	= output record = $y(t)$
$Y(f)$	= finite Fourier transform of output $y(t)$
$Y^*(f)$	= complex conjugate of $Y(f)$

$y(t)$	= output record = x_{q+1}
γ_{ij}^2	= ordinary coherence function of x_i and x_j ($i \neq j$)
γ_{ij-r}^2	= partial coherence function ($i \neq j$)
$\gamma_{xy}^2(f)$	= ordinary coherence function of input $x(t)$ and output $y(t)$
γ_{yx}^2	= multiple coherence function
δ_{dlc}	= weighted direct lift control flap (aircraft input signal)
δ_e	= elevator (aircraft input signal)
δ_H	= horizontal stabilizer (aircraft input signal)
δ_{TR}	= pedals (helicopter input signal)
δ_x	= longitudinal stick (helicopter input signal)
δ_y	= lateral stick (helicopter input signal)
δ_0	= collective lever (helicopter input signal)

Introduction

MULTIPLE-INPUT/-OUTPUT (MIMO) analysis procedures for linear systems are known in theory,¹⁻⁵ but very little is known in their general applications to flight test data. In practical situations, the measured inputs/outputs are generally correlated and it is necessary to identify the spectral nature of multiple inputs and also to evaluate their separate and combined effects on any selected output. This information is useful in the design, testing, and control of flight vehicles that must operate in a dynamic environment. Ordinary coherence functions have been extensively applied in studying single-input/-output (SISO) relations of missiles, spacecraft, aircraft, acoustics, and industrial machinery in the frequency domain. These results are used in assessing the validity of the frequency response functions from measured data, in eliminating redundant data channels, and in detecting potential nonlinearities. Ordinary coherence functions and associated coherent output spectra have been shown to give still useful and reliable information about systems involving several inputs and outputs that are not mutually correlated. These systems can be treated as a collection of SISO models. On the other hand, when MIMO channels are correlated, for instance in aircraft and helicopter dynamics, the ordinary coherence functions alone fail to separate out the coupled spectral effects of different control inputs, e.g., aileron/rudder coupling on the output spectra of yaw/roll rate, and fail also to distinguish their individual frequency response functions. Use of ordinary coherence functions by itself in these applications will give er-

Received Jan. 28, 1989; revision received and accepted for publication June 11, 1990. Copyright © 1990 by the American Institute of Aeronautics and Astronautics, Inc. All rights reserved.

*Assistant Director, Flight Mechanics and Controls Division, Post Bag No. 1799; currently Guest Scientist, Deutsche Forschungsanstalt für Luft- und Raumfahrt, Institut für Flugmechanik, Postfach 3267, D-3300 Braunschweig, Germany.

†Group Leader, Software Development Group, Mathematical Methods and Data Handling Branch, Institut für Flugmechanik, Postfach 3267.

roneous results and incorrect interpretation of input/output relations.

Although a matrix approach to the solution of MIMO systems has been discussed by Otnes and Enochson,³ this approach, unfortunately, is computationally laborious, needs inversion of spectral matrices in complex arithmetic at every frequency point, and does not allow spectral separation for sequential inspection of input/output relationships.

Dodds and Robson⁶ obviated this difficulty to some extent by introducing the concept of partial coherence functions, which in conjunction with ordinary coherence functions sheds tremendous physical insight into the interpretation of the coupled spectral nature of stationary random processes. Based on this idea, Bendat⁷⁻⁹ described computationally efficient iterative procedures that involve conditioning to separate out the linear coupling effects. Special quantities of interest such as partial and multiple coherence functions, conditioned frequency response functions, and coherent output spectra were derived to provide greater engineering insight into the physical meaning of various input/output relationships. These, in fact, form the powerful tools for system identification in the frequency domain. Barrett and Halvorson¹⁰ have used these techniques to determine the dynamic excitation sources on launch vehicle payloads as a three-input/single-output problem. Recently, Tischler¹¹ has studied the coupled roll/yaw response of XV-15 tilt-rotor aircraft due to control deflections from aileron/rudder combinations by treating the problem as a two-input/single-output system. More recently, Tischler and Fletcher¹² have used matrix-based multiple-input/single-output (MISO) procedures to extract accurate mathematical models of a BO-105 helicopter as a four-input/one-output problem. These models have been validated and compared favorably against the time-domain approach followed by Kaletka and Grünhagen.¹²

In the present paper, Bendat's iterative techniques have been adopted to develop a computer program and illustrate their utility in aircraft and rotorcraft applications. The results are presented by considering flight test data from two research vehicles of the DLR Braunschweig, a BO-105 helicopter and the inflight simulator ATTAS (Advanced Technologies Testing Aircraft System), and illustrated with applications from conventional SISO systems to MISO systems with up to four simultaneous correlated inputs. Specific applications studied are the following: 1) the detection of extraneous noise at the output caused by a smaller number of control inputs (BO-105 helicopter), 2) investigation of control buildup at the output level (BO-105 helicopter), and 3) the investigation of the influence of the autotrim system of the in-flight simulator ATTAS on its direct lift control flaps.

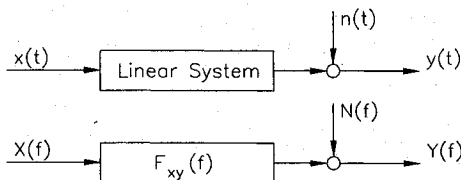


Fig. 1 Single-input/single-output system.

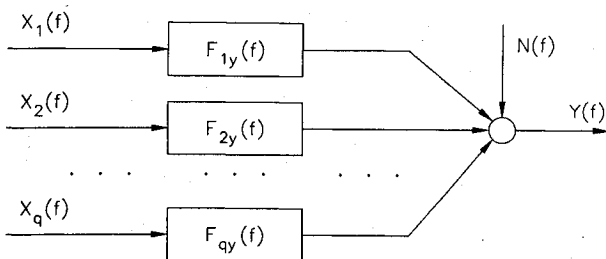


Fig. 2 Multiple-input/single-output system.

Theoretical Background

In the treatment of SISO problems (Fig. 1), it is generally considered that the input/output records $x(t)$ and $y(t)$, respectively, are measured realizations of stationary random processes and assumed that the input time record is noise free and the output time record contains extraneous noise such as contributions from unknown, unmeasured, or other than selected input; nonlinear effects of the dynamic system; time delay errors; statistical and computational errors; nonstationary effects; instrument noise; and any other errors that cause the measured output to deviate from the true output.

The system is described in the frequency domain by a set of spectral, coherence, and frequency response functions

$$S_{xx}(f) = \frac{1}{T} X^*(f)X(f) \quad (1)$$

$$S_{yy}(f) = \frac{1}{T} Y^*(f)Y(f) \quad (2)$$

$$S_{xy}(f) = \frac{1}{T} X^*(f)Y(f) \quad (3)$$

$$\gamma_{xy}^2(f) = \frac{|S_{xy}(f)|^2}{S_{xx}(f)S_{yy}(f)} \quad (4)$$

$$F_{xy}(f) = \frac{S_{xy}(f)}{S_{xx}(f)} \quad (5)$$

where $X(f) = X(f, T)$, $Y(f) = Y(f, T)$ are the finite Fourier transforms (length T) of the simultaneously measured input/output channels $x(t)$ and $y(t)$, the $*$ denoting the complex conjugate.

MISO problems (Fig. 2) with inputs that are not mutually coherent can be treated as simple SISO systems. With mutually coherent inputs, such treatment gives incorrect estimation of the spectra. Bendat⁷⁻⁹ has shown how such systems can be handled by removing the linear coupling effects between the inputs and the outputs by a process that is called conditioning of the given model (Fig. 3). Such a process would

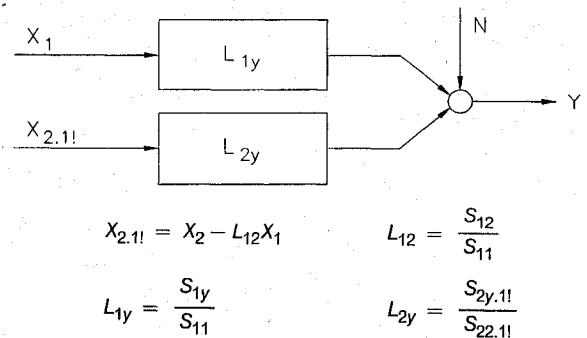


Fig. 3 Conditioned input/output model.

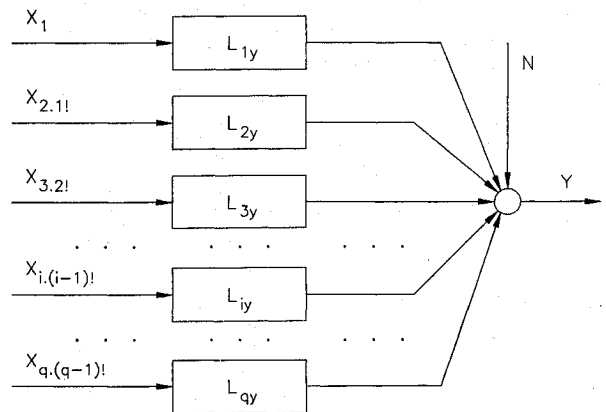


Fig. 4 Conditioned multiple-input/single-output system.

then generate conditioned multiple-input/single-output (CMISO) systems (Fig. 4) that can be decomposed into a set of noninterference conditioned single-input/single-output (CSISO) systems to give more meaningful and correct information about the spectral nature and the physical relationships between input and output. These are described by Bendat by a set of interrelated computationally efficient iterative algorithms to compute ordinary and conditioned input/output records; ordinary, partial, and multiple coherence functions; ordinary and conditioned spectral density functions; ordinary and conditioned frequency response functions; and decomposition of measured output spectra into separate contributions from several inputs and the rest from extraneous noise. These algorithms have been used by the present authors to develop a computer program for arbitrary q inputs and one output and illustrate their utilities in study of practical problems.

General Computational Algorithms

If $\{x_i(t)\}$ ($i = 1, 2, \dots, q$) represent q distinct simultaneously measured input records and $x_{q+1}(t) = y(t)$ represents the simultaneously measured output, then by following Bendat's notation, the generalized algorithm is compactly described in the following:

Step 0

Compute spectral density functions S_{ij} between q inputs and the output for $i, j = 1, 2, \dots, q + 1$ by

$$S_{ij} = \frac{1}{T} X_i^* X_j \quad (i \leq j) \quad (6)$$

Compute the ordinary coherence functions by

$$\gamma_{ij}^2 = \frac{|S_{ij}|^2}{S_{ii} S_{jj}} \quad (i < j) \quad (0 \leq \gamma_{ij}^2 < 1) \quad (7)$$

Compute frequency response functions by

$$L_{ij} = \frac{S_{ij}}{S_{ii}} \quad (1 < j) \quad (8)$$

Step r

Compute conditioned spectral density functions for $i, j = r + 1, \dots, q + 1$ ($i \leq j$)

$$\begin{aligned} S_{ii \cdot r} &= S_{ii \cdot (r-1)} - |L_{ri}|^2 S_{rr \cdot (r-1)} \\ &= S_{ii} (1 - \gamma_{ri}^2) (1 - \gamma_{2i \cdot 1}^2) \dots (1 - \gamma_{ri \cdot (r-1)}^2) \end{aligned} \quad (9)$$

$$S_{ij \cdot r} = S_{ij \cdot (r-1)} - L_{rj} S_{ir \cdot (r-1)} \quad (i < j) \quad (10)$$

Compute partial coherence functions by

$$\gamma_{ij \cdot r}^2 = \frac{|S_{ij \cdot r}|^2}{S_{ii \cdot r} S_{jj \cdot r}} \quad (i < j) \quad (11)$$

and compute conditioned frequency response functions by

$$L_{rj} = \frac{S_{rj \cdot (r-1)}}{S_{rr \cdot (r-1)}} \quad (2 \leq r < j) \quad (12)$$

If $r = q$, then compute noise spectrum by

$$S_{nn} = S_{yy} (1 - \gamma_{1y}^2) (1 - \gamma_{2y \cdot 1}^2) \dots (1 - \gamma_{qy \cdot (q-1)}^2) \quad (13)$$

compute multiple coherence function by

$$\gamma_{y \cdot x}^2 = 1 - (1 - \gamma_{1y}^2) (1 - \gamma_{2y \cdot 1}^2) \dots (1 - \gamma_{qy \cdot (q-1)}^2) \quad (14)$$

and decompose output spectrum by

$$\begin{aligned} S_{yy} &= |L_{1y}|^2 S_{11} + |L_{2y}|^2 S_{22 \cdot 1} + \dots + \\ &\quad |L_{qy}|^2 S_{qq \cdot (q-1)} + S_{nn} \\ &= \gamma_{1y}^2 S_{yy} + \gamma_{2y \cdot 1}^2 S_{yy \cdot 1} + \dots + \\ &\quad \gamma_{qy \cdot (q-1)}^2 S_{yy \cdot (q-1)} + S_{nn} \end{aligned} \quad (15)$$

The right side of Eqs. (15) contains $q + 1$ terms, the first q of which represents, respectively, the coherent output spectrum due to the q -ordered conditioned inputs, and the last term is the noise spectrum. The utility of this representation of output spectra has been shown for each of the examples considered on a BO-105 helicopter and ATTAS aircraft. It may be observed here that conditioning the spectral density functions in Eqs. (9) and (10) is comparable to that of triangularization of a spectral density function matrix of Gaussian elimination type. Conditioning of frequency response functions in Eq. (12) corresponds to the use of pivotal row elements at each stage of the elimination. This analogy greatly simplifies the coding procedure.

Computational Aspects

In the same manner as satisfied by the spectral density functions, their conditioned forms also satisfy similar relations for $i = 1, 2, \dots, q + 1$; $j = 2, 3, \dots, q + 1$ and $r < i$:

$$S_{ii \cdot r} \geq 0 \quad S_{ij \cdot r} = S_{ji \cdot r}^* \quad (16)$$

$$S_{ii} \geq S_{ii \cdot 1} \geq S_{ii \cdot 2} \geq \dots \geq S_{ii \cdot r} \quad S_{yy} \geq S_{yy \cdot 1} \geq$$

$$S_{yy \cdot 2} \geq \dots \geq S_{yy \cdot r} \quad (17)$$

Similarly, partial coherence functions satisfy

$$\gamma_{ii \cdot r}^2 = 1, \quad \gamma_{ij \cdot r}^2 = \gamma_{ji \cdot r}^2 \quad (i \neq j) \quad (0 \leq \gamma_{ij \cdot r}^2 < 1) \quad (18)$$

For the algorithm and the program to be stable, certain numerical bounds have to be defined for frequency domain functions. In view of the inequality in Eqs. (16), a suitable lower bound for spectral estimates S_{ii} has to be set. In view of Eqs. (9) used in Eqs. (11) and (12), an upper bound for coherence functions has to be set. These settings are enough to fix the lower bounds of conditioned autospectral density functions as these can be expressed in terms of the original autospectral density functions S_{ii} and coherence functions, as shown in Eqs. (9). For the results presented, a maximum value of ordinary, partial, and multiple coherence functions is set to 0.99999 in each case and a minimum value of autospectral estimates is set to 1.0×10^{-30} as parameters. In the matrix approach, the failure of the inequality conditions at certain frequency points corresponds to inversion of singular spectral density matrices. Thus, the breakdown of the algorithm in this approach is repeatedly overcome by suppressing these frequency points, which are not known a priori. However, in the present approach, this problem has been fully overcome by defining the proper bounds for spectral and coherence estimates as above.

For optimization of computer storage, the spectral density function matrix $S = (S_{ij})$ can successively be overwritten at each step. Similar storage optimization can be done for coherence and frequency response functions. For computation of two-sided spectral density functions alone in complex arithmetic for q ordered inputs and one output it is sufficient to have $n(q + 1)^2$ locations, where n is the number of points of the selected time record and the frequencies being limited to $0 \leq f_k \leq f_c$, where f_k and f_c are the intermediate and the Nyquist cutoff frequencies, respectively.

For q arbitrary inputs, there exist $q!$ models. As Otnes and Enochson³ have discussed, the computational accuracy and



Fig. 5 Helicopter BO-105.



Fig. 6 Aircraft ATTAS.

Table 1 Input/output channels

Input/output	Name	Data channel
Helicopter input		
δ_x	DELTA _X	Longitudinal stick
δ_y	DELTA _Y	Lateral stick
δ_{TR}	DELTA _{HR}	Pedals
δ_0	DELTA ₀	Collective lever
Helicopter output		
p	P	Roll rate
Aircraft input		
δ_e	RETA	Elevator
δ_H	RHS	Horizontal stabilizer
δ_{dlc}	RLD	Weighted direct lift control flap
Aircraft output		
a_z	RAZS	Normal acceleration

results depend on the order in which the control inputs are selected. To get a physically meaningful model, ordering of the inputs is necessary. The input record that exhibits highest coherence in the desired frequency range was selected as the first record. Ordering of the remaining records was done on similar argument. For instance, in the helicopter example, the time history record of lateral control input was chosen as the first record in preference to that of longitudinal stick input in view of its highest coherence to output roll rate. The mean values of input/output records were subtracted before fast Fourier transforms were computed. The resulting spectral quantities were smoothed by a moving average procedure with an appropriate number of points before they were conditioned by the general algorithm.

Application to Flight Test Data

For the purposes of illustration and demonstrating the usefulness of the method, some practical examples formulated in terms of MISO systems from flight records of instrumented helicopter BO-105 and ATTAS aircraft VFW-614 are considered here. Table 1 shows the list of input/output data channels.

The BO-105 helicopter (Fig. 5), which has a highly coupled dynamic system, is controlled by four pilot inputs, namely, longitudinal stick δ_x for pitch, lateral stick δ_y for roll, pedals δ_{TR} for yaw, and collective lever δ_0 for heave control. The positions of the controls are indicated as a percentage of their movement for quantification. The limits $\pm 100\%$ denote the right or left positions of the pedals or the lateral stick and push or pull position of the longitudinal stick. The collective stick is limited from 0 to 100%. Similarly, the in-flight simulator ATTAS (Fig. 6) has an elevator δ_e for pitch, ailerons for roll, and rudder for yaw control. Additionally, ATTAS is equipped with direct lift control (DLC) flaps for direct lift control and an autotrim system.

Let us consider flight test data of the BO-105 conducted in practically calm air with an indicated air speed of about 60 kt in a density altitude of about 2500 ft (Fig. 7). This test was specially designed for system identification purposes both in time and frequency domain. System identification means extrac-

tion of physically defined aerodynamic and flight mechanics parameters from flight test measurements. These parameters, referred to as stability derivatives, are the coefficients in the mathematical model that closely describes the characteristics of the dynamics of the system. Such parameters are considered to be more reliable since they are estimated from the measurements of the flying vehicle. Therefore, accurate formulation of the mathematical model and, hence, extraction of parameters is the most important step in system identification. The identification is done from two approaches, namely, time and frequency domain, with a view to verify and have faith in the model for its suitability in different applications, namely simulation validation, control system design (in particular, a model of the control system for inflight simulation), handling qualities criteria, etc. Such a step often becomes mandatory as the model is extracted from a small number of flight tests. Both of these approaches need a model structure and require a careful consideration of what effects are to be included or eliminated for successful identification. For example, in the case of the BO-105, because of its stiff rotor system with a relatively large hinge offset, the control stick inputs δ_y , δ_x , δ_{TR} , δ_0 are coupled, so that a classical separation of longitudinal and lateral motion, as found in aircraft, becomes inappropriate. Therefore, it is important to investigate whether each of the control inputs has an effect on the response variables before the model is formulated. Any unmodeled terms at this stage reflect as extraneous noise and degrade the accuracy of the model. By conducting multivariable spectral analysis, it is shown how the multiple coherence function is enabled to detect the noise and how the quality of the model is improved when each of the control inputs progressively is accounted. Whereas this is one of the important issues in time-domain identification, the key step in frequency-domain identification procedure is to extract frequency response functions between each pair of input/output to which appropriate transfer function models are fitted for identifying the system. These functions ideally must be free from contaminated effects, both at the input and output levels. Therefore, such effects must be removed both at input and output to obtain high-quality frequency response functions before models are fitted. It is shown how such a function can be extracted when there is a control coupling between δ_y and δ_x . In the other two sections, the utility of the spectral decomposition of the output is illustrated by the investigation of the control buildup (BO-105) and of the influence of the autotrim system of the inflight simulator (ATTAS) on its DLC flaps. We enumerate the applications in the following.

Application of Multiple Coherence Function

Single-Input/Single-Output System—Conventional Theory

Suppose the helicopter stick control inputs δ_y and δ_x with output roll rate p (Fig. 7) are analyzed as two separate SISO systems, SISO 1 and SISO 2, respectively, then we have the ordinary coherence functions γ_{py}^2 (Fig. 8) and γ_{px}^2 (Fig. 9) as a measure of the accuracy of the frequency response functions F_{1y} and F_{2y} .

Two-Input/Single-Output System—Importance of Conditioning

Now, the computation of the ordinary coherence function γ_{12}^2 (Fig. 10) shows that there is a control coupling between δ_y and δ_x . Therefore, by the foregoing theory, considering this as a two-input/single-output problem, the partially contaminated effect of δ_y is removed from both δ_x and p to obtain conditioned input/output spectral density functions $S_{22,1!}$ and $S_{yy,1!}$.

Since $0 \leq \gamma_{12}^2 < 1$ and $0 \leq \gamma_{1y}^2 < 1$, it can be shown that $S_{22,1!} = S_{22}(1 - \gamma_{12}^2) \leq S_{22}$, $S_{yy,1!} = S_{yy}(1 - \gamma_{1y}^2) \leq S_{yy}$, indicating the use of contaminated spectra S_{22} and S_{yy} at the input and output in place of $S_{22,1!}$ and $S_{yy,1!}$ while considering

SISO 2. The extent to which these are contaminated by the effect of δ_y is shown in Figs. 11 and 12. Consequently, the gain and phase representation of the frequency response function L_{2y} for the conditioned SISO 2 varies from F_{2y} , and this is represented in a Bode diagram (Fig. 13). Its accuracy is measured by the partial coherence function $\gamma_{2y,1!}^2$ (Fig. 9), which also indicates the extent to which the roll rate p may be predicted from δ_x , when linear effects of δ_y are removed from both δ_x and p . These functions are regarded to be more valid and accurate than F_{2y} (Fig. 13) and γ_{2y}^2 (Fig. 9) in the optimal least squares prediction sense as discussed by Bendat.⁸ Kaletka et al.¹² have used this concept to identify conditioned fre-

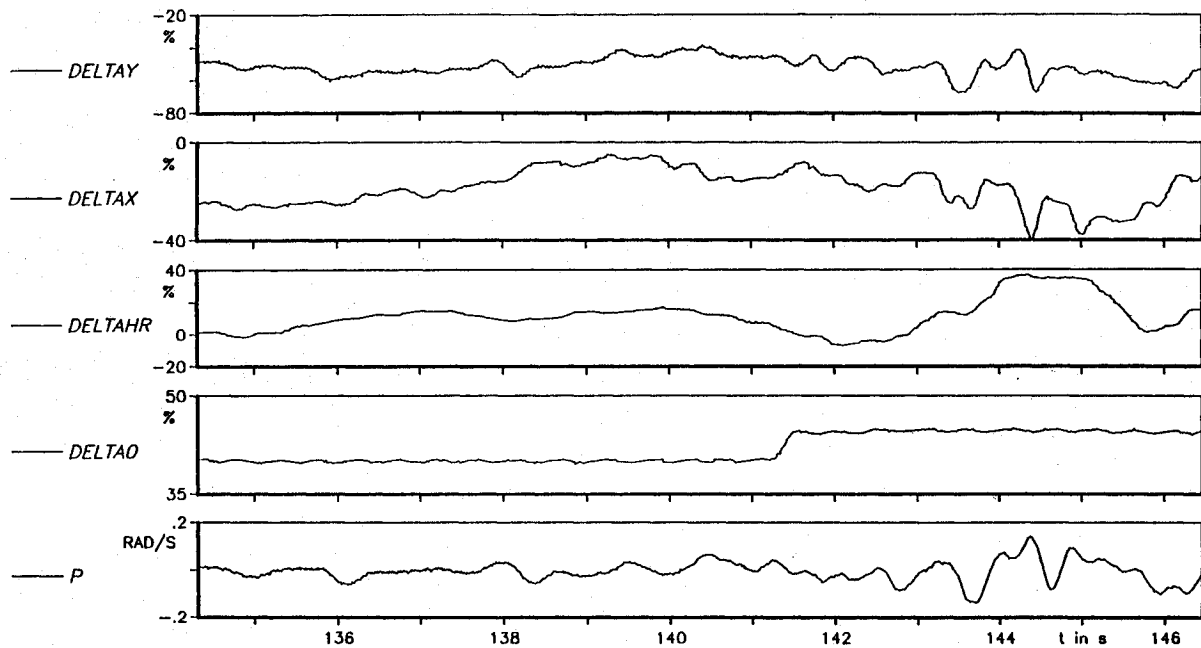


Fig. 7 Helicopter flight test data.

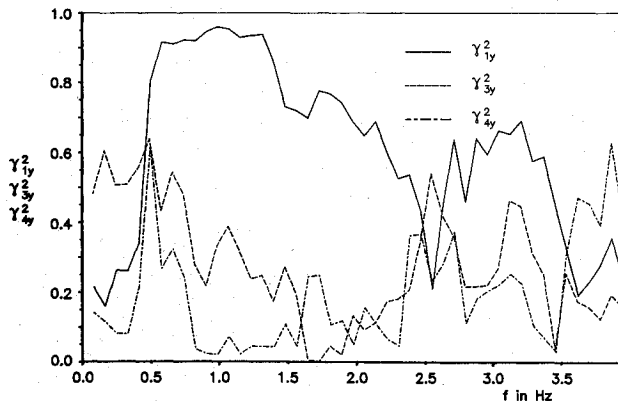


Fig. 8 Ordinary coherence functions.

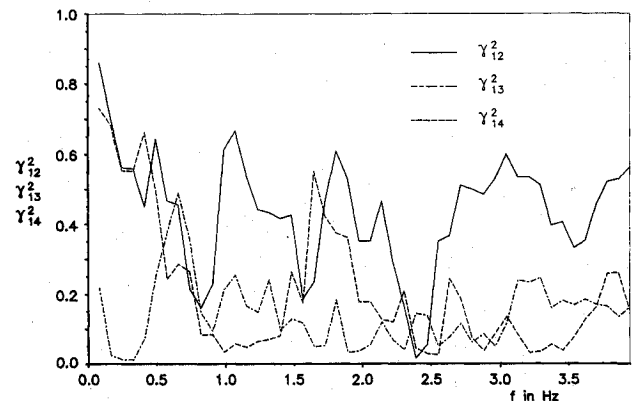


Fig. 10 Control coupling.

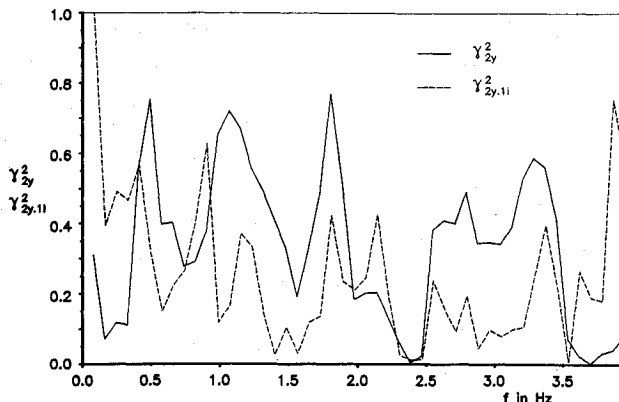


Fig. 9 Ordinary and partial coherence functions.

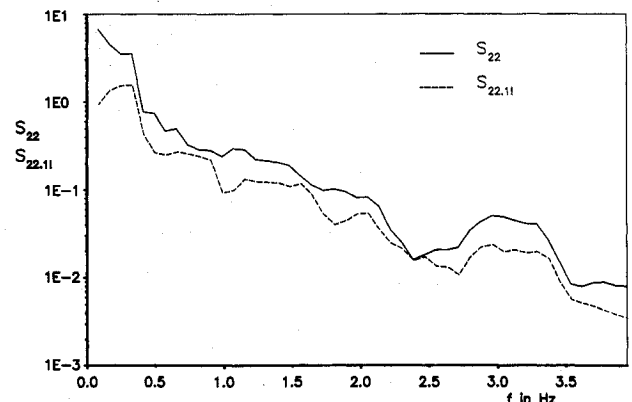


Fig. 11 Ordinary and conditioned input spectra.

quency response functions from BO-105 data and validate them from the time-domain approach. Thus, by the process of conditioning, one can study a realistic transfer function behavior from one control to one state. This establishes the importance of conditioning correlated input/output systems.

Three-Input/Single-Output Systems—Importance of Multiple Coherence Functions

The multiple coherence function $\gamma_{y:x}^2$ (Fig. 14) due to the combined influence of two control inputs δ_y and δ_x alone exhibits a moderate relationship to the roll rate p and indicates the probable influence of other inputs that have to be investigated. The computation of the ordinary coherence function γ_{3y}^2 (Fig. 8) indicates that the third control input, tail rotor δ_{TR} , is a strong contributor to this observation and, hence, it cannot be neglected. Thus, if we separate out the mutual influences between δ_y , δ_x , and δ_{TR} and then take their combined influence on p , a considerable improvement in the multiple co-

herence function $\gamma_{y:x}^2$ and reduction in noise to output signal ratio can be seen from Fig. 14.

Four-Input/Single-Output Systems—Detection of Extraneous Noise Due to Fewer Inputs

Now, if we proceed further to take the influence of the collective lever δ_0 as the fourth input, which is coupled with δ_y , δ_x , and δ_{TR} , then again a remarkable improvement in the multiple coherence function $\gamma_{y:x}^2$ and, hence, in the reduction in the noise to output signal ratio can be seen from Fig. 14. This result shows how well the multiple coherence function can help in the detection of extraneous noise caused by fewer inputs and indicates that all four inputs contribute to roll rate response p and have to be considered in the model formulation. Additionally, since the multiple coherence has attained values closer to unity over a broad frequency range, this shows that the total roll rate p can be linearly accounted for by considering all four pilot inputs. Also, $\gamma_{y:x}^2$ indicates that the turbulence and nonlinear effects are not significant in this response.

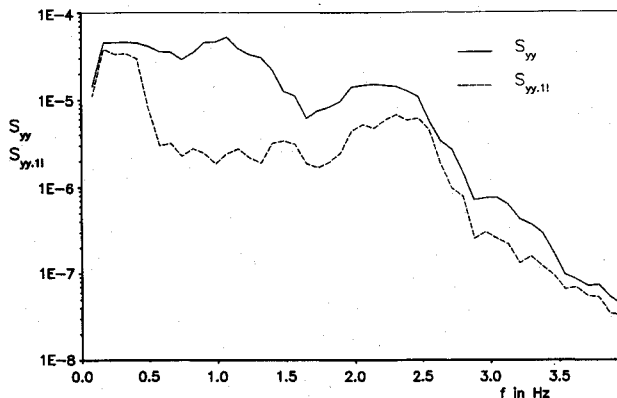


Fig. 12 Ordinary and conditioned output spectra.

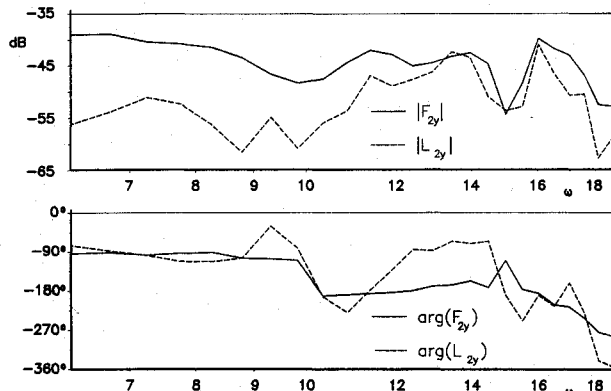


Fig. 13 Frequency response functions.

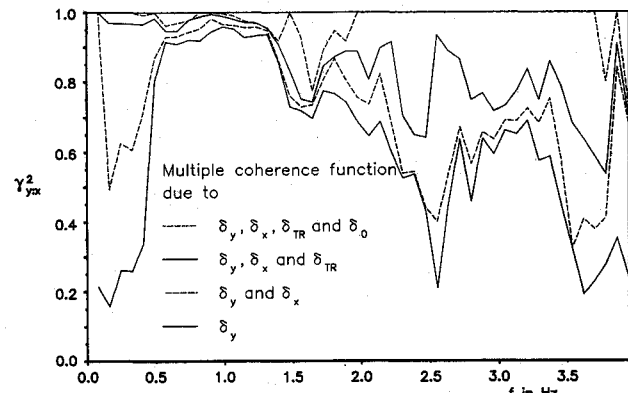


Fig. 14 Multiple coherence functions.

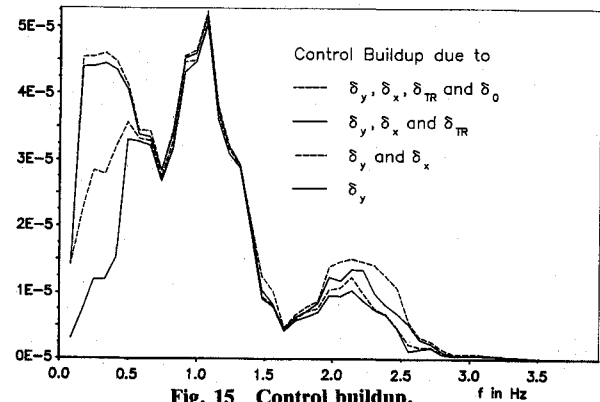


Fig. 15 Control buildup.

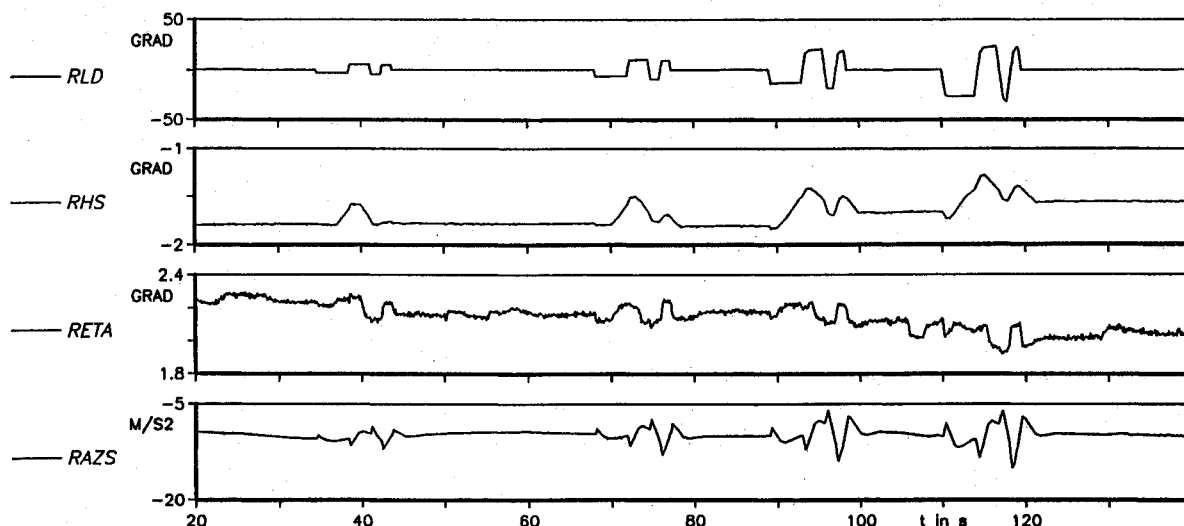


Fig. 16 Aircraft flight test data.

Application of Decomposition of Output Spectra

Control Buildup—BO-105 Helicopter

One of the most important pieces of design information for the control systems engineer is to estimate how much of spectral output is due to the various control inputs and how they are built up at the output when the effect of each control input is included. This is illustrated by considering again the same flight maneuver of the BO-105 helicopter wherein all the four control inputs are excited (Fig. 7). Treating the task as a four-input/one-output problem, the spectral output of roll rate p has been decomposed into physical meaningful contributions from control inputs δ_y , δ_x , δ_{TR} , and δ_0 , and unknown extraneous noise. The control buildup at the output (Fig. 15) is shown by spectral output due to δ_y alone; combined spectral output due to δ_y and δ_x ; combined spectral output due to δ_y , δ_x , and δ_{TR} ; and combined spectral output due to δ_y , δ_x , δ_{TR} , and δ_0 . The figure shows that the major portion of the control buildup in the frequency range 0.5–1.5 Hz comes from the lateral stick δ_y , as predicted from the coherence function γ_{1y}^2 (Fig. 8).

Influence of Autotrim System on Direct Lift Control Flaps—ATTAS Aircraft

Let us consider another example to study the influence of the autotrim system of ATTAS on the effectiveness of DLC flaps, which is characterized by the normal acceleration. This is illustrated by the decomposition of the output spectrum of the normal acceleration. The research aircraft ATTAS (Fig. 6), which has been equipped with onboard high-speed computers and a modern fly-by-wire system, is built to the needs of present and future technological demands in many application areas like flight planning, flight control, air traffic control, and studies of new control systems; it is also used as a flying simulator. In addition, ATTAS is equipped with an autotrim system to reduce the stick force, so that the safety pilot of ATTAS can take over in any event of failure of the fly-by-wire system without hardship. This system works on the principle of reducing the hinge moments between elevator and horizontal stabilizer by suitably deflecting them without altering the trim lift of the horizontal tail. However, these deflections, which are computed through an algorithm from the onboard computer, may not be accurate, possibly either due to inaccuracies in the table of values stored in the computer relating to hinge moments as a function of several aerodynamic factors (change in angle of attack, speed of the aircraft, downwash due to change in deflection from DLC or landing flaps, etc.), or to assumptions made in the computational algorithm connecting the relationship between control surface movements to the autotrim system's deflections or to any other reasons. Thus, these variations caused by the autotrim system may influence undesirable aerodynamic effects, i.e., the loss of effectiveness of DLC flaps, and therefore, the investigation of its influence is important.

To illustrate this, the response of normal acceleration at c.g. due to the deflection of DLC flaps δ_{dlc} together with the

deflection of elevator δ_e and horizontal stabilizer δ_H caused by the autotrim system is considered here from ATTAS flight test data (Fig. 16) measured at an altitude of about 19,000 ft with an indicated air speed of about 140 kt. Considering this as a three-input/single-output problem, the output spectrum of a_z has been decomposed to yield the following: coherent output spectrum due to the DLC flaps, coherent output spectrum due to the horizontal stabilizer, coherent output spectrum due to the elevator, and output noise spectrum.

It can now be seen that the contribution to the output normal acceleration is maximum from the DLC flaps (Fig. 17), whereas the contributions from δ_H and δ_e are negligible. Thus, these results show that there is no significant loss of effectiveness of the DLC flaps due to the autotrim system, which is a desirable criterion. The summation of the coherent output spectra together with the output noise spectrum to yield the original measured autospectrum of the normal acceleration is done to provide an overall check on the extensive computations performed.

Conclusions

The practical utilities of MISO methods have been illustrated by considering helicopter and aircraft flight test data. The procedure is iterative, computationally efficient, and allows the sequential/combined inspection of coupled systems. The method provides useful information about the physical understanding of vehicle dynamics and is quite promising in system identification analysis. It is believed that, with the availability of these techniques, interest in the frequency-domain analysis approach is further enhanced, considering the advantage that they provide solutions with no assumptions made on the model order.

Acknowledgments

The authors gratefully acknowledge the director of the National Aeronautical Laboratory, R. Narasimha, and the director of the DLR Institute for Flight Mechanics, P. Hamel, for their encouragement. The authors also gratefully acknowledge their colleagues from the Institute for Flight Mechanics for suggesting practical applications. The authors are also thankful to the associate editor and the reviewers for their constructive suggestions.

References

- Jenkins, G. M., and Watts, D. G., *Spectral Analysis and Its Applications*, Holden-Day, San Francisco, CA, 1968.
- Koopmans, L. H., *The Spectral Analysis of Time Series*, Academic Press, New York, 1974.
- Otnes, R. K., and Enochson, L., *Applied Time Series Analysis*, Wiley, New York, 1978.
- Bendat, J. S., and Piersol, A. G., *Engineering Applications of Correlation and Spectral Analysis*, Wiley, New York, 1980.
- Bendat, J. S., and Piersol, A. G., *Random Data: Analysis and Measurement Procedures*, 2nd ed., Wiley, New York, 1986.
- Dodds, C. J., and Robson, J. D., "Partial Coherence in Multivariate Random Processes," *Journal of Sound and Vibration*, Vol. 42, No. 2, 1975, pp. 243–249.
- Bendat, J. S., "Modern Analysis Procedures for Multiple Input/Output Problems," *Journal of the Acoustical Society of America*, Vol. 68, No. 2, 1980, pp. 498–503.
- Bendat, J. S., "System Identification from Multiple Input/Output Data," *Journal of Sound and Vibration*, Vol. 49, No. 3, 1976, pp. 293–308.
- Bendat, J. S., "Solutions for the Multiple Input/Output Problem," *Journal of Sound and Vibration*, Vol. 44, No. 3, 1976, pp. 311–325.
- Barrett, S., and Halvorson, R. M., "The Use of Coherence Functions to Determine Dynamic Excitation Sources on Launch Vehicle Payloads," NASA CR-3142, June 1979.
- Tischler, M. B., "Frequency-Response Identification of XV-15 Tilt-Rotor Aircraft Dynamics," NASA TM-89428, May 1987.
- Kaletka, J., von Grünhagen, W., Tischler, M. B., and Fletcher, J. W., "Time and Frequency-Domain Identification and Verification of BO 105 Dynamic Models," *Proceedings of the Fifteenth European Rotorcraft Forum*, Amsterdam, The Netherlands, Sept. 1989, pp. 66-1-66-25.

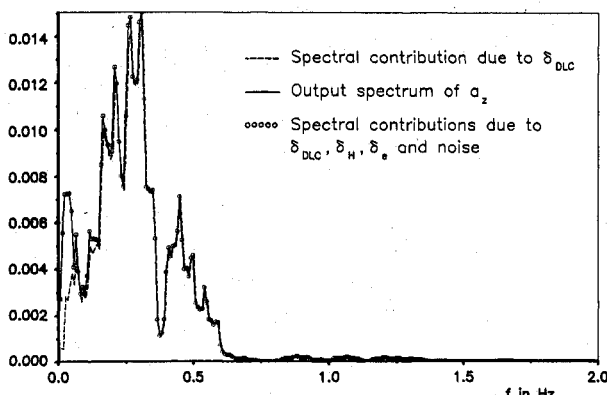


Fig. 17 Decomposition of output spectra.